

# Aqueous Phase Photochemistry of $\alpha$ -Keto Acids as a Function of pH

Michael Ryan Dooley

Department of Chemistry and Biochemistry

University of Colorado at Boulder

March 21 2017

Advisor: Dr. Veronica Vaida, Department of Chemistry and Biochemistry

Committee:

Dr. Veronica Vaida, Department of Chemistry and Biochemistry

Dr. Robert Parson, Department of Chemistry and Biochemistry

Dr. Chris Bowman, Department of Chemical and Biological Engineering

## Tables of Contents

Abstract.....	page 2
Introduction.....	page 2
Experimental Methods.....	page 9
Materials.....	page 9
Titration – Debye-Huckel Extended Method.....	page 9
Photolysis of Pyruvic Acid.....	page 11
Ultraviolet-Visible Spectroscopy.....	page 12
<sup>1</sup> HNMR.....	page 12
Electrospray Ionization Mass Spectrometry.....	page 13
Results and Discussion.....	page 13
Determination of Acid Dissociation Constants.....	page 13
Dependence of Keto-Diol Ratio on pH.....	page 16
Dark Processing of Pre-Photolysis Solutions.....	page 18
Photolysis of Pyruvic Acid.....	page 21
Conclusions and Future Directions.....	page 27
References.....	page 29

## Abstract

$\alpha$ -Keto acids react in solution in the presence of sunlight to form complex organic oligomers that can contribute to the formation of organic atmospheric aerosols. The sunlight-initiated reactions of two  $\alpha$ -keto acids, pyruvic acid and 2-oxooctanoic acid, were studied under a range of pH's from 2.35 to 11 to determine how their photochemical reactivity was affected by changing reaction conditions. The acid dissociation constants of both acids in aqueous solution were determined by titration, yielding a  $pK_a$  of  $2.51 \pm 0.05$  for pyruvic acid and  $2.49 \pm 0.04$  for 2-oxooctanoic acid. The photolysis was conducted using a solar simulator, and the progress of the reaction was monitored with UV-vis and NMR spectroscopy in addition to electrospray ionization mass spectrometry. As the pH of the reaction solution was increased, the rate of the photolysis of pyruvic acid was shown qualitatively to slow down. Additionally, the relative yields and the ratios of products generated from the photolysis of pyruvic acid were observed to be dependent upon the pH of the reaction solution. This has important implications for the fate of  $\alpha$ -keto acids in the natural environment, where chemistry occurs in media with a range of differing acidities.

## Introduction

Atmospheric aerosols are solid or liquid particles suspended in air. Aerosols play an important role in climate, by scattering solar and terrestrial radiation.<sup>1</sup> They have also been implicated in epidemiological studies of human health.<sup>2, 3</sup> In addition, aerosol particles limit visibility in the natural environment.<sup>4</sup> Atmospheric aerosols can be generated by wind action on the sea-surface, as shown in Figure 1.<sup>5</sup> It has now been established by atmospheric measurements that organic compounds are important constituents of atmospheric aerosols and affect their formation, growth, and optical and chemical properties.<sup>6-8</sup> Organic aerosols can be formed either directly (primary organic aerosol, POA) or generated by further reactions of volatile organic matter that can be found in the air (secondary organic aerosols, SOA) either in the gas or the particle phase.<sup>9</sup> Photochemical reactions of small organic molecules in the aqueous phase that generate bigger molecules by the formation of carbon-carbon bonds are of particular interest.<sup>7, 10-</sup>

In nature, aqueous environments are found with a wide range of acidities. For example, the ocean is basic with a pH of  $\sim 8$ . However, the pH of aerosols, even those generated from sea spray, changes due to reactions with gases in the atmosphere, such as  $\text{SO}_2$ ,  $\text{NO}_2$ , and  $\text{CO}_2$ . These gases react with water to produce corresponding acids ( $\text{H}_2\text{SO}_4$ ,  $\text{HNO}_3$ , and  $\text{H}_2\text{CO}_3$ , chemistry shown in Figure 1) and then dissociate, influencing the pH in aqueous aerosol phase.<sup>16</sup> Such changes in pH affect organic molecules within the aerosol, particularly the extent of protonation and hydration of a given molecule.

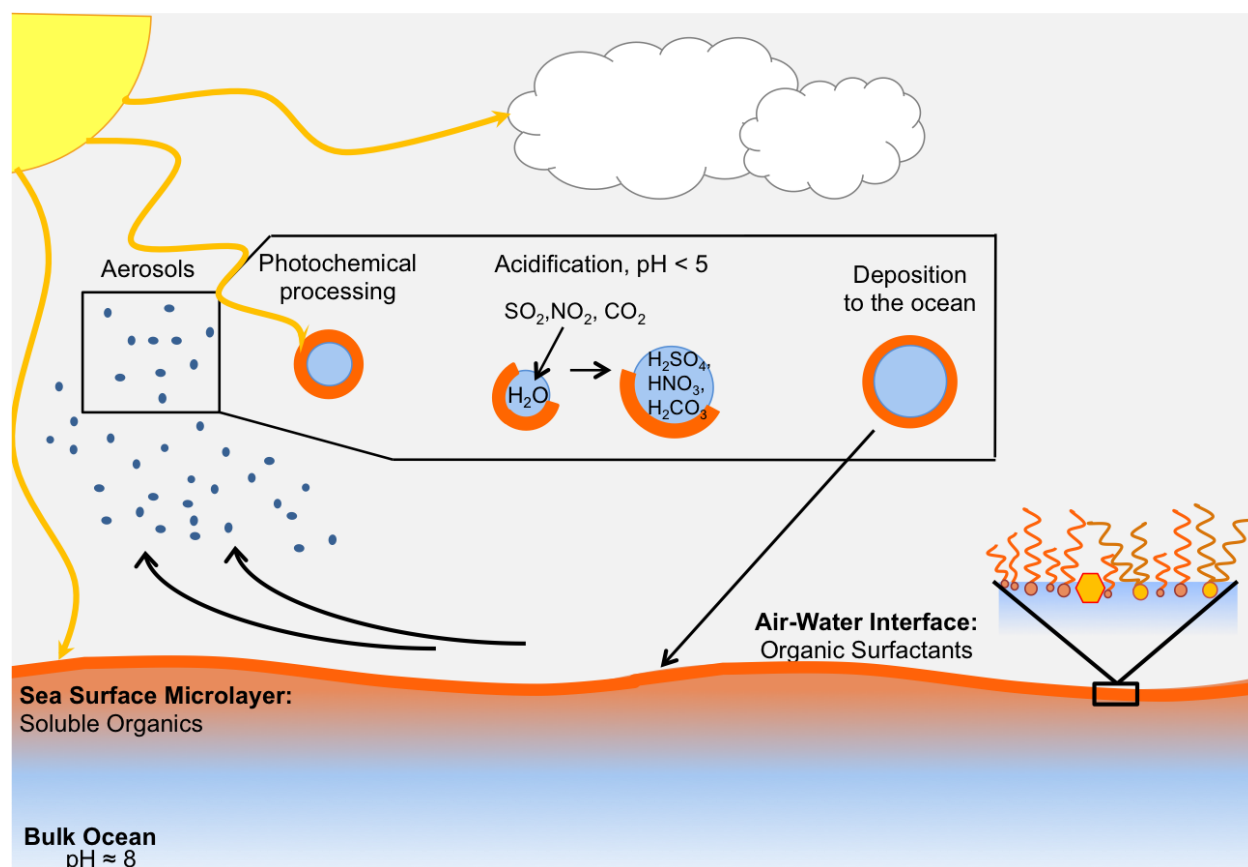


*Figure 1. Illustration of the formation and processing of aqueous organic aerosols (organic material is shown in orange) in the environment, including the acidification of aerosols by the formation of acids from the reaction of gases with the water in the aerosol.*

One such class of organic molecules is  $\alpha$ -keto acids, which are found in both the gas and aqueous phase in the atmosphere and are recognized to be important in atmospheric chemistry.<sup>17</sup> Pyruvic acid, the simplest  $\alpha$ -keto acid, is found in the natural environment both in the condensed phase (in aerosols, fogs, and clouds), as well as in the gas phase. Its fate in the atmosphere is determined by its absorption of solar radiation and subsequent photochemical reactions, rather

than by oxidation with hydroxyl radical.<sup>18</sup> Pyruvic acid has also been used as a model system to understand the fate of related more complicated  $\alpha$ -dicarbonyl species in the atmosphere.

Pyruvic acid undergoes both gas phase photochemistry and aqueous phase reactions.  $\alpha$ -Keto acids with a longer alkyl chain, such as 2-oxooctanoic acid (2-OOA), are less volatile, but are also of interest because they still undergo the same reactivity in the aqueous phase. In the aqueous phase, these reactions often form a carbon-carbon bond, generating oligomers, thus building molecular complexity. These products are particularly interesting due to their low vapor pressure and apparent ability to contribute to SOA formation in the atmosphere.<sup>10, 13</sup> Consequently, it is important to study rates and products of their reactions as a function of pH.

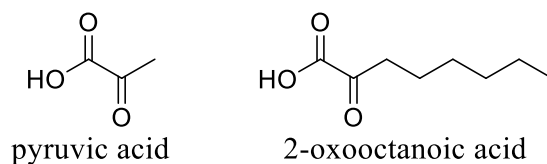


*Figure 2. Structure of pyruvic acid and 2-oxooctanoic acid.*

In this study, we aim to understand the photochemistry in the aqueous phase of pyruvic acid and 2-OOA as a function of pH (structures shown above in Figure 2). The Vaida group has studied extensively the photochemical reactions of aqueous pyruvic acid and 2-OOA at low pH,<sup>10-13, 19</sup> but very little is known about the reactivity of  $\alpha$ -keto acids at higher pH. In 1963, Leermakers and Vesley observed that the rate of photolysis of pyruvic acid is slowed considerably when the solution pH is raised to 6.1,<sup>20</sup> but other than this brief mention there is no literature on this subject. I hypothesize that, because changing the pH of the solution affects the extent of both the hydration and deprotonation of  $\alpha$ -keto acids, raising the pH of the reaction solution will affect the branching ratio of the observed photoproducts, in addition to slowing the rate of photolysis. Consequently, I have investigated the photochemistry of pyruvic acid in aqueous solution across a range of pH from 2 to 11 in detail, as well as performing initial studies on the effect of pH on the photo reactivity of 2-OOA.

In aqueous solution, pyruvic acid and 2-OOA are found as keto acids in equilibrium with their hydrated, geminal diol forms (2,2-dihydroxypropanoic acid, 2,2-DHPA, Figure 3).<sup>21</sup> At a low pH, it is easier to hydrate the pyruvic acid because the reaction is efficiently catalyzed by acids. The diol form is also more abundant at low pH. Conversely, the keto form is more

common at a high pH. This equilibrium has a significant effect on the photolysis reaction because the keto form absorbs near-UV light, but the diol form does not absorb light within the atmospherically-relevant wavelength range. This means that in the environment only the keto form can absorb sunlight to initiate photochemical reactions.

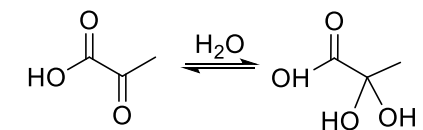


*Figure 3. Equilibrium of pyruvic acid between its keto and its diol, 2,2-dihydroxypropanoic acid (2,2-DHPA,) conformers.*

Additionally, as a function of pH, organic acids deprotonate, in the case of pyruvic acid forming the conjugate base, pyruvate (Figure 4). At low pH most of the pyruvic acid exists in the protonated state, whereas at high pH most of the compound is in the deprotonated form, pyruvate.

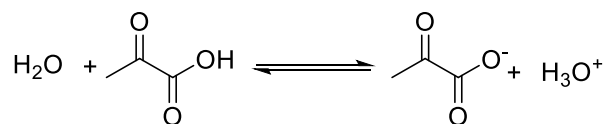


*Figure 4. Pyruvic acid dissociation equilibrium.*

In this study, the photolysis of pyruvic acid is examined as a model for the larger class of  $\alpha$ -keto acids. In the natural environment, pyruvic acid is first electronically excited by UV light from the Sun to the first singlet excited state. In aqueous solution, it is possible to undergo intersystem crossing to the reactive triplet excited state,  $^3(\text{n}, \pi^*)$ . This photoexcited molecule then undergoes a hydrogen abstraction reaction with another ground state pyruvic acid molecule, in either the keto or diol form, generating reactive radical species. The radicals can then recombine in solution, often forming a carbon-carbon bond and oligomeric species.

The commonly accepted mechanism for the aqueous phase photolysis of pyruvic acid at unadjusted pH (2.35), as determined by the Vaida group, is shown in the scheme in Figure 5 below.<sup>11, 12, 14</sup> This reaction scheme starts with hydrogen abstraction from a ground state pyruvic acid molecule (Reaction 2), leading to the formation of reactive radical species. Figure 5 shows the triplet state interacting with the diol conformer. The hydrogen abstraction step of the reaction can, in principle, occur from any hydrogen on the molecule in either the keto or diol conformer.

At low pH, the diol form of pyruvic acid is abundant in solution, and it has been shown that it is energetically favorable to hydrogen abstract from the diol conformer.<sup>14</sup> Taken together, this suggests that the triplet excited state likely first reacts with the diol form of pyruvic acid in solutions that have not been pH adjusted. The major product generated following this reaction scheme is dimethyltartaric acid (DMTA), as shown in Reaction 4. DMTA is the major observed photoproduct in solutions that have not been pH adjusted.<sup>11</sup>

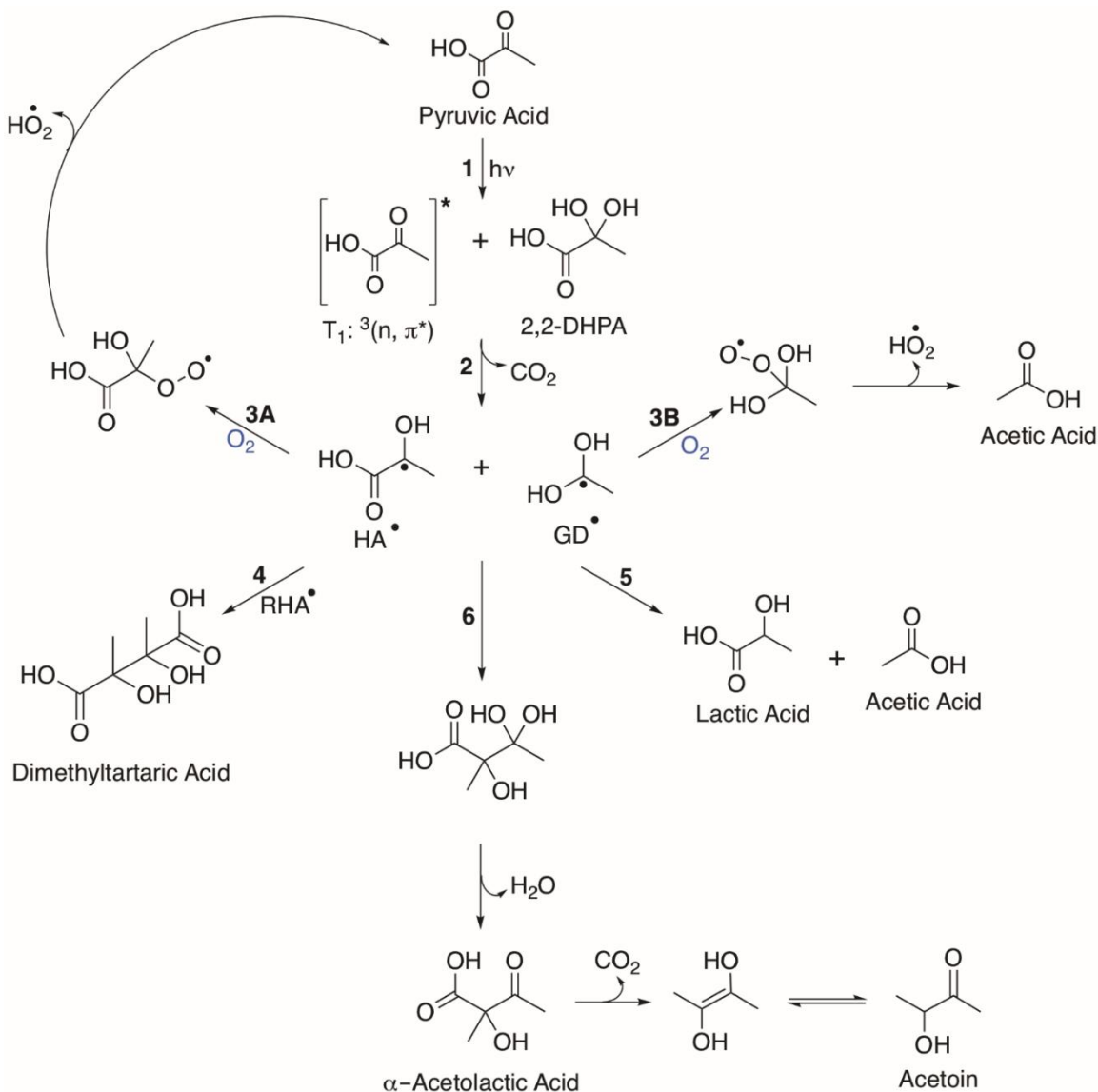
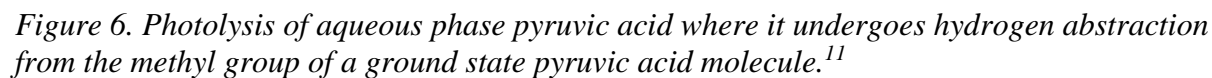


Figure 5. Photolysis of aqueous phase pyruvic acid where it undergoes hydrogen abstraction from the carboxyl group of a ground state pyruvic acid molecule (shown here in the diol conformer).<sup>11</sup>



This parapyruvic acid is itself photoreactive, and is readily available to react in the photolysis solution because it has the same  $\alpha$ -keto functionality as pyruvic acid. Figure 7 below illustrates how parapyruvic acid can undergo photochemical excitation and crossreact with a pyruvic acid molecule to eventually form 2,4-dihydroxy-2-methyl-5-oxohexanoic acid (DMOHA), which is observed as an important oligomeric photoproduct even at unadjusted pH.<sup>11</sup>



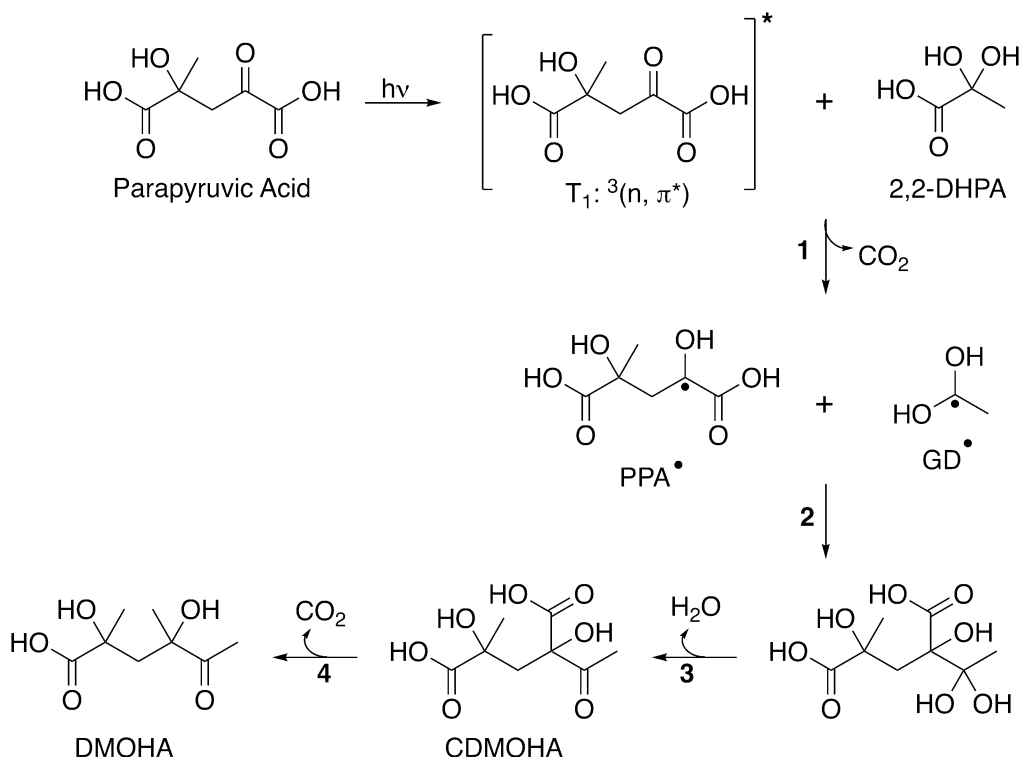


Figure 7. Photochemical reaction scheme of aqueous parapyruvic acid.<sup>11</sup>

DMOHA is observed as an important photoproduct even at the low pH of the unadjusted solutions of pyruvic acid. However, per this scheme, one would expect the branching ratio to shift to favor DMOHA even more at high pH. At high pH the ratio of keto to diol shifts to favor the keto conformer. In the literature, it is reported that photolysis of pyruvic acid proceeds more slowly at higher pH,<sup>20</sup> which might not be expected given that more of the photoactive keto conformer is present. However, this may be explained because hydrogen abstraction is energetically favored from the diol form.<sup>14</sup> However, this observed change in kinetics does not account for the new reaction pathways outlined in Figures 6 and 7. At higher pH there should be more keto conformer of pyruvic acid and when the keto conformer is deprotonated, the methyl group is the only available site for hydrogen abstraction. Because of this, I hypothesize that the pH of the solution influences the branching ratio of major observed products of the photolysis reaction. The relative yields of major photoproducts are likely dependent on the ratio of keto-diol form. This ratio is dependent on pH, and, therefore, it is possible that the major product generated by the photolysis of pyruvic acid can be determined by the pH of the reaction solution, shifting to favor DMOHA over DMTA at higher pH.

## Experimental Methods

### Materials:

Pyruvic acid (98%, Sigma-Aldrich) was distilled twice under reduced pressure (< 1 Torr) while heating gently (< 55 °C). 2-Oxo-octanoic acid (>99%, Sigma-Aldrich) was used without further purification. All solutions were made using 18.2 MΩ water (3 ppb TOC), and the pH of solutions was adjusted using stock solutions of 1 M NaOH (98.0%, Fischer Scientific).

### Titration – Debye-Huckel Extended Method

The effective acid dissociation constants were determined for both pyruvic acid and 2-OOA by titrating 10 mM pyruvic acid and 3 mM 2-OOA with 15 mM and 10 mM NaOH solutions, respectively. The pH measurements were taken using an electronic pH probe, Corning pH meter 320. For each experiment the probe was calibrated using standard buffer solutions at pH 4, 7, and 10. After calibrating the machine, the pH probe was cleaned and placed in the sample in question where it could equilibrate. Then the pH was recorded continuously during the titration experiments.

An extended version of the Debye-Huckel method of determining  $pK_a$  from a plot of pH versus NaOH was used to calculate the acid dissociation constants, following the fitting routine given in Harris's *Quantitative Chemical Analysis* textbook<sup>22</sup> with modifications to account for ionic strength taken from Papanastasiou and Ziogas 1995.<sup>23</sup> The  $pK_a$  was calculated using an iterative fitting routine described below. This allowed us to calculate the  $pK_a$  using the full range of data, unlike other methods, such as Gran plots that use only data from the exponential part of the curve.<sup>22</sup>

First, a list of proton concentration for each data point of the titration is calculated using equation 1.

$$\text{Equation 1: } 10^{-pH} = [H^+]$$

Next, the values of this list of proton concentrations, in addition to the constant  $K_w$ , which depends on temperature, are used to calculate a list of hydroxide concentrations for each data point using equation 2.

$$\textbf{Equation 2: } [OH^-] = \frac{K_w}{[H^+]}$$

The Debye-Huckel coefficient for the acid,  $\alpha_{HA}$ , was then calculated for each data point using equation 3.

$$\textbf{Equation 3: } \alpha_{HA} = \frac{K_a}{[H^+] + K_a}$$

The value  $\phi$  can be solved for using equation 4 and then can be used to find the volume of base added for each step of the titration,  $V_b$ , using equation 5.

$$\textbf{Equation 4: } \phi = \frac{\alpha \frac{H^+ - OH^-}{C_a}}{1 + \frac{H^+ + OH^-}{C_b}}$$

$$\textbf{Equation 5: } V_b = \phi \times C_A \times \frac{V_a}{C_b}$$

These  $V_b$  values were then plotted against the pH. For dilute solutions of acid, the addition of NaOH can significantly affect the overall ionic strength of the solution, which can in turn influence the experimental  $pK_a$  value. Therefore, the ionic strength was calculated using equation 6 for each point of the titration.

$$\textbf{Equation 6: } I = [H^+] + C_b$$

This ionic strength value,  $I$ , is then used to calculate an effective activity coefficient,  $y_i$ , using the Debye-Huckel equation. The  $\log(y_i)$  can be calculated using equation 7, where  $A$  and  $B$  are constants that depend on the physical properties of the solution. For our solutions, we used the values for water at room temperature,  $A = 0.5085$ ,  $B = 0.3281$ . The effective diameter of the ion,  $\text{\AA}$ , was taken to be 5 angstroms.<sup>23</sup>

$$\textbf{Equation 7: } \log(y_i) = -\frac{A\sqrt{I}}{1 + B\text{\AA}\sqrt{I}}$$

Equation 8 calculates the  $y_i$  value.

$$\textbf{Equation 8: } y_i = 10^{\log(y_i)}$$

Using these activity coefficients a corrected list of proton concentrations was calculated for each point of the titration, using equation 9.

$$\text{Equation 9: } [H^+] = \frac{\alpha_H}{y_i}$$

Using this initial list of corrected proton concentrations and an initial guess for the value for the  $K_a$ , the residuals were calculated using equation 10 and then summed together. The offset given in equation 10 accounts for the presence of deprotonated molecules prior to the addition of any base, treating the deprotonation of these molecules as if some amount of base had been already added to the system.

$$\text{Equation 10: } \text{Residual} = [(V_b + \text{offset}) - V_{\text{predicted}}]^2$$

The data was then fit by reducing this sum of residuals using the Microsoft Excel solver function, allowing the base offset, acid concentration, and  $K_a$  to vary. By minimizing the residuals, it is possible to extract a  $K_a$  that best fits the entire experimental data set.

### Photolysis of Pyruvic Acid

A 450 W Xenon arc lamp was used as a solar simulator. The photolysis cell was purged with  $N_2$  gas to remove the oxygen from the cell. The oxygen is removed to prevent the pyruvic acid from regenerating during the reaction (as in Reaction 3A of Figure 5) and slowing the generation of oligomeric photoproducts.<sup>11, 12</sup>

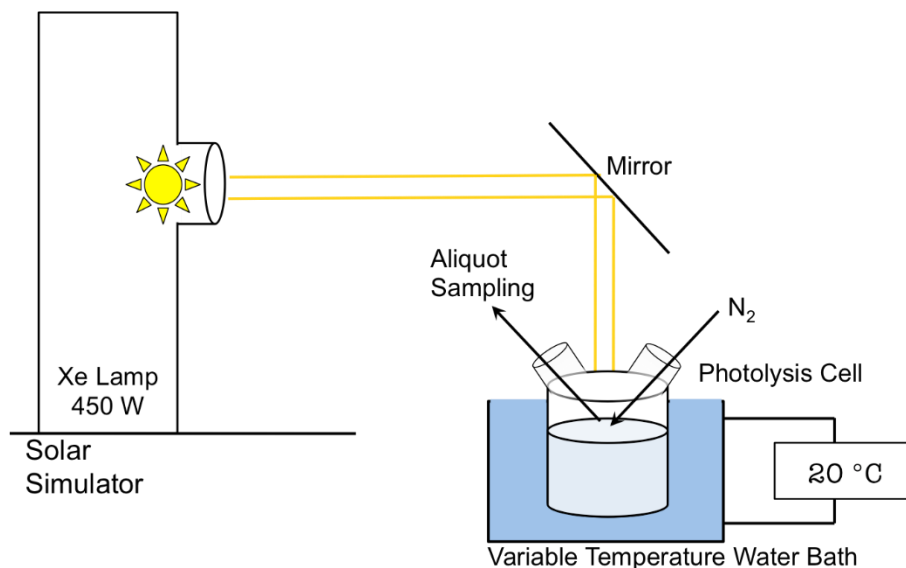


Figure 8. Illustration of photolysis cell and Xe lamp

The reaction cell was filled with 250 mL of the pyruvic acid solution at 10mM and then the quartz window bolted on. The cell has inlets for two needles. The first was used to take aliquots. The second was used to flow nitrogen into the cell. The nitrogen being pumped in was pushed through a Teflon tube so that it bubbled through the solution to purge the cell of oxygen. A syringe placed next to this without any attachment acted as a consistently-sized relief valve. The nitrogen was bubbled through the cell beginning one hour before the lamp was turned on each time and continuing for the duration of the experiment to remove oxygen, which can react with the excited states of the acids. A chiller and water bath were used to maintain the desired temperature at 20 °C sample for the duration of the experiment. An aliquot of the solution was removed before photolysis began as a dark control and kept in the dark at room temperature. Because solutions at different temperatures can have different pH measurements, the photolysis was conducted at roughly room temperature. 10 mL Aliquots were also collected at 1 hour intervals during photolysis. The reaction cell was exposed to light from the solar simulator for five hours, after which point it was turned off. The pre-photolysis solution, the aliquots, and the post photolysis solution were all examined by UV-vis spectroscopy and electrospray ionization mass spectrometry.

### **Ultraviolet Visible Spectroscopy**

A Cary 5000 was used for UV-vis spectroscopic analysis. Quartz cuvettes used for samples were cleaned before each scan with methanol and then Milli-Q water. A blank cuvette of Milli-Q water was used for the baseline and the Cary 5000 was used in double beam mode. For each of the photolysis reactions, the aliquots, post-hv sample, and pre-hv sample UV spectra were collected. The pre-photolysis control solution was scanned at the beginning of the experiment and then additionally every hour. The data interval was set to 0.5 nm. The instrument was used with the baseline correction option on. The scan rate was 300 nm/minute and the spectral range was 200-800 nm. The concentration of the samples is the same as for photolysis, 10 mM.

### **<sup>1</sup>H NMR**

Proton NMR spectra were obtained using a Varian INOVA-500 NMR operating at 499.60 MHz for <sup>1</sup>H observation. In order to perform <sup>1</sup>H detection in aqueous solution, temperature was held at 23°C and an optimized WET pulse sequence was utilized to eliminate >99% of the H<sub>2</sub>O signal<sup>8</sup>. The pH of the pyruvic acid solutions was changed using 10 mM NaOH solution.

## Electrospray Ionization Mass Spectrometry

The pyruvic acid photolysis solutions were also examined in a Waters Synapt G2 HDMS mass spectrometer to assess the products formed during the reaction. Mass spectrometry scans were taken of aliquots corresponding to several timepoints for each photolysis reaction, including the pre- and post-photolysis solutions. In mass spectrometry, the species present need to be ionized to be observed, so additional preparation is needed to ionize the molecules in the sample. Samples were diluted 1:1 with methanol, and negative electrospray ionization (ESI<sup>-</sup>) was employed to ionize the products. Negative mode was chosen because the species in the solution are mostly acidic, meaning that it is easier to remove hydrogens from such species than add them (as would be required in positive mode) using electrospray ionization. The mass spectrometry results show the mass to charge ratios ( $m/z$ ) of the species present in the solution. Under the ionization conditions used, it is expected that primarily singly charged species will be observed. The ESI<sup>-</sup> MS experiments conducted were not designed to be absolutely quantitative, and no calibration curve was prepared. However, for similar solutions the number of counts on the mass spectrometer can be compared with each other to evaluate the presence and, qualitatively, the relative abundance of photoproducts.

## Results and Discussion

In order to determine how changes in pH might affect the photochemical reactivity of  $\alpha$ -keto acids, it is necessary first to understand how the precursor behaves in aqueous solutions of varying acidity. The pre-photolysis solutions of pyruvic acid and, in some cases, 2-OOA were characterized, including determining the acid dissociation constant for both acids. Changes in the keto-diol ratio and the absorption spectra were also investigated, as was the formation of oligomers via dark processes. Following the characterization of the initial starting solutions, the photolysis of pyruvic acid as a function of pH was studied using both UV-vis spectroscopy and electrospray ionization mass spectrometry.

### Determination of Acid Dissociation Constants

After several repeated titrations, values for the effective  $pK_a$  of pyruvic acid and 2-oxooctanoic acid were determined to be  $2.51 \pm 0.05$  and  $2.49 \pm 0.04$ , respectively. The simple titration method used here can only determine an effective  $pK_a$ . This is because the measured pH

of the solution reflects the overall dissociation for the mixture of diol and keto forms that are present in solution. The keto and diol conformers individually have different  $pK_a$  values. For pyruvic acid, the keto conformer has a reported  $pK_a$  value of 2.18, while the diol has a reported value of 3.6.<sup>24</sup> However, the  $pK_a$  of mixture of the two conformers that exists in aqueous solution is, perhaps, the more relevant quantity. The value obtained by our experiments,  $2.51 \pm 0.05$ , is in good agreement with the literature value of 2.49.<sup>25</sup>

Unlike pyruvic acid, the  $pK_a$  value for 2-OOA is not well known. There is only one report in the literature, which gives a value of 2.78,<sup>26</sup> higher than that found here. However, this may be due to the fact that the value reported in the literature did not account for the changing ionic strength of the solution during the titration, as done here. Our confidence in the experimental value of the  $pK_a$  of 2-OOA obtained here is, in part, due to how well our experimental results matched the literature value for pyruvic acid. The good agreement between the effective  $pK_a$  values of pyruvic acid and 2-OOA also makes sense due to the similarity between the two molecular structures. We conclude that the length of the alkyl tail has little influence on the  $pK_a$  of  $\alpha$ -keto acids. These two values are both precise and accurate, meaning the extended Debye-Huckel iterative fit method was successful. Figures 9 and 10 show example titration data for both pyruvic acid and 2-OOA, along with the corresponding fit curve used to extract the  $pK_a$  value. Both show how well the calculated curve fits the experimental data. The method used to fit the titration data here of an ionic strength correction combined with the extended Debye-Huckel model can be used to determine values of  $pK_a$  with accuracy. With this method, the effective  $pK_a$  of other  $\alpha$ -keto acids with differing alkyl chain lengths could also be easily determined.

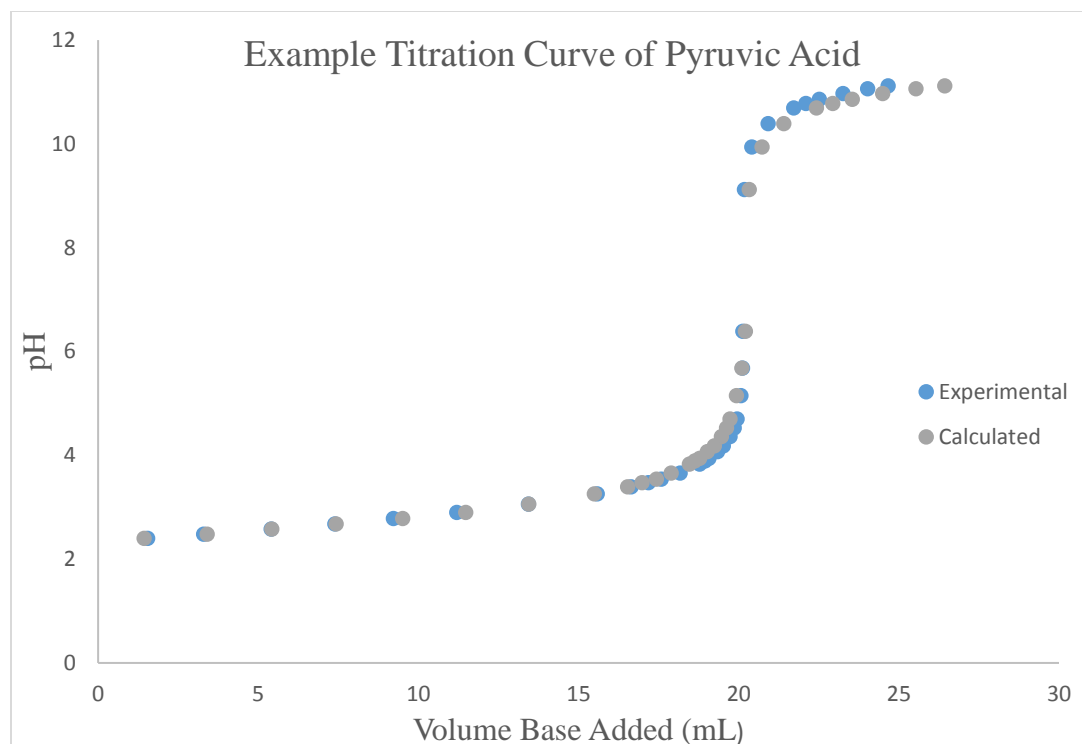


Figure 9. Example experimental titration curve of pyruvic acid (blue) and the calculated curve (grey).

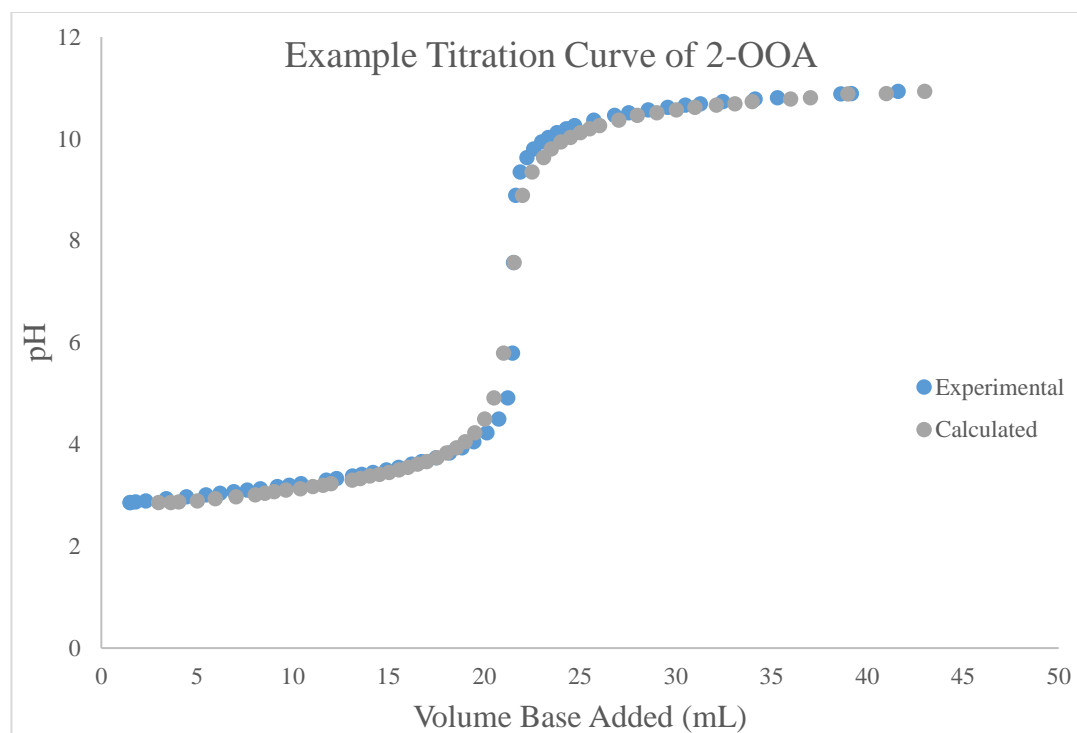


Figure 10. Example experimental titration curve of 2-OOA (blue) and the calculated curve (grey).



## Dependence of Keto-Diol Ratio on pH

Q-HNMR was used to measure the ratio of keto to diol form as a function of pH. Table 1 shows the percentage of pyruvic acid in the diol form at the indicated pH. For 10 mM solutions of pyruvic acid at unadjusted pH, pyruvic acid exists almost equally in both the keto and diol conformer. However, even a relatively modest increase in pH lowers the amount of diol in solution significantly, confirming that the pH influences the ratio of keto to diol conformers. It also suggests that at higher pH much more keto form will be available to form parapyruvic acid and eventually DMOHA, as predicted.

*Table 1. Percent pyruvic acid in diol form as a function of pH.*

<b>pH of solution</b>	<b>Percent pyruvic acid in diol form</b>
2.31	47.9%
4.31	11.8%
5.24	11.6%
7.01	11.6%
10.46	9.3%

The increase in the relative ratio of keto to diol conformer at high pH may also explain the changes observed in the UV absorption spectra of both pyruvic acid and 2-OOA as pH is increased. For both pyruvic acid (Figure 11) and 2-OOA (Figure 12) the absorbance increases as pH is increased. This stronger absorbance as a function of pH is likely because more keto form is present in the high pH solutions than in the unadjusted solutions. Only the keto forms of  $\alpha$ -keto acids are chromophores that will contribute to this absorption, and it is unlikely that deprotonation changes the electronic structure of the keto conformer very much. Thus, at high pH, a higher absorbance is seen.

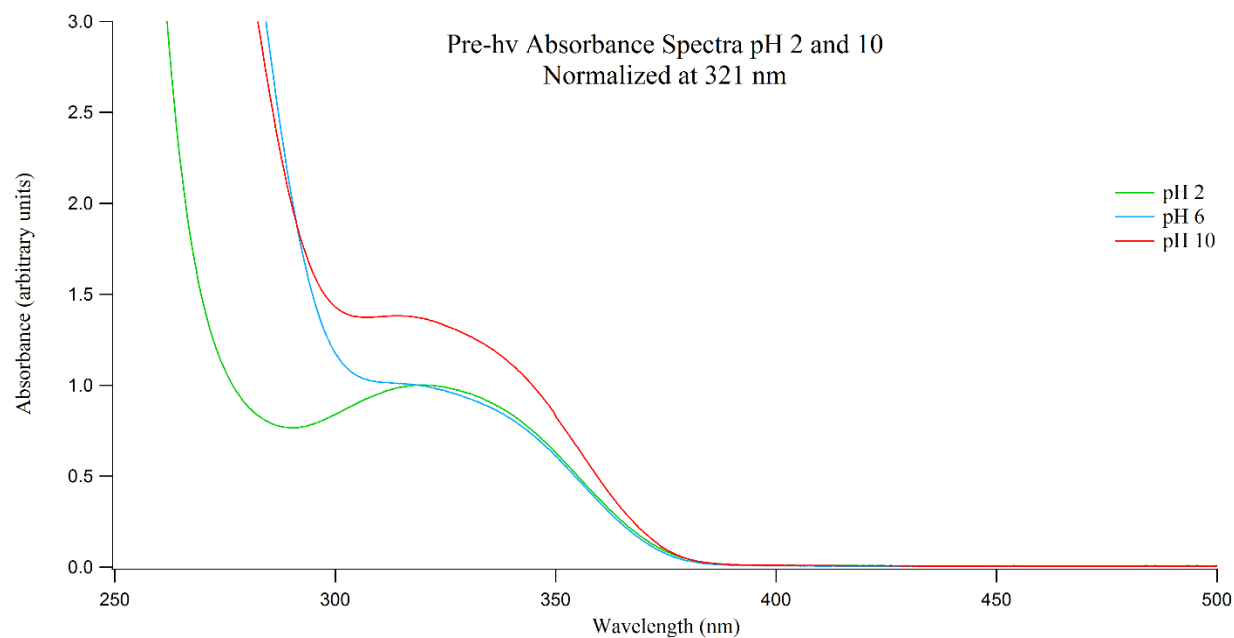


Figure 11. UV-vis spectra of 10 mM pyruvic acid solutions at pH values 2 (unadjusted, green), 6 (blue), and 10 (red) with absorption scaled by concentration and normalized.

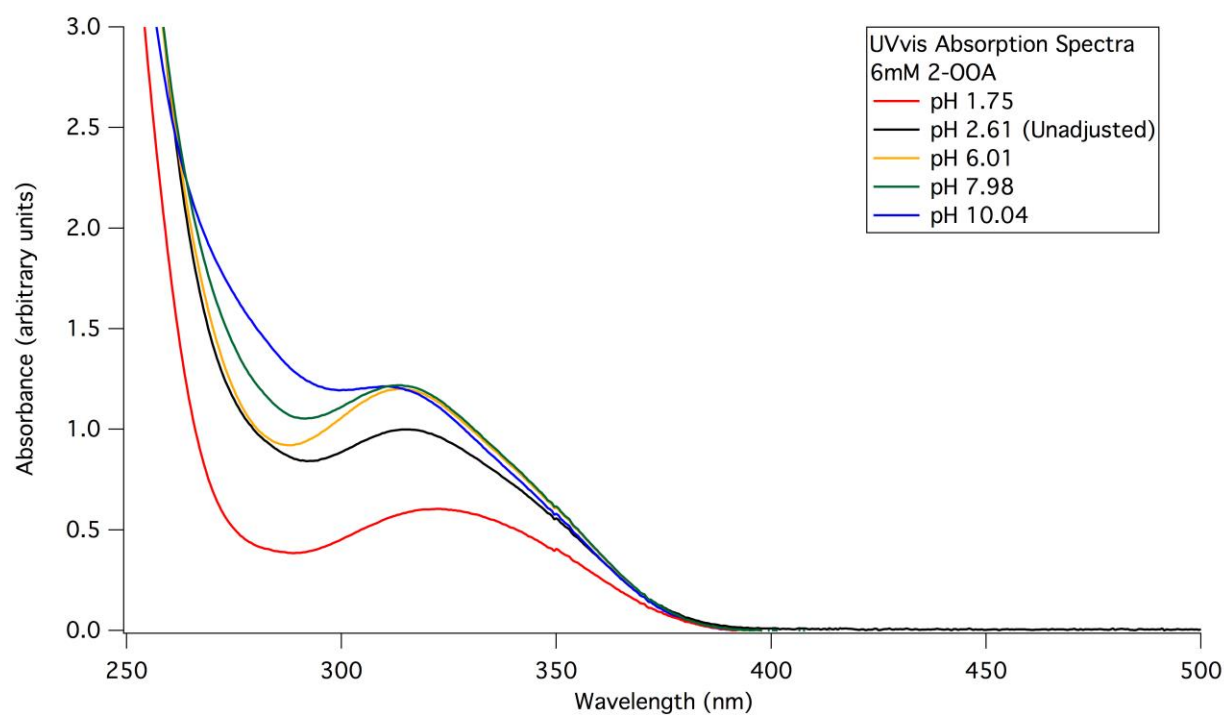


Figure 12. UV-vis spectra of 6 mM 2-OOA solutions at pH values 1.75 (red), 2.61(unadjusted, black), 6.01 (yellow), 7.98 (green), and 10.04 (blue) with absorption scaled by concentration and normalized.

Figure 13 shows the UV absorption of pyruvic acid in aqueous solution at unadjusted pH as well as the spectral irradiance of the solar spectrum near the surface of the Earth<sup>27</sup> and the absolute irradiance of the unfiltered 450 W Xe arc lamp used in the photolysis experiment. There is a strong overlap between the pyruvic acid absorption and the spectral output of the experimental and natural light source. This confirms the wavelengths required to initialize this reaction are available in both our experimental and natural environmental conditions. Unlike the solar spectrum observed near the surface of the Earth,<sup>27</sup> which is filtered by the ozone layer, the unfiltered Xe arc lamp also contains higher energy UV light, extending beyond 290 nm. Previous results in the Vaida lab have shown that, while this additional light increases the observed rate of the reaction, it does not change the observed photochemical products.<sup>12</sup>

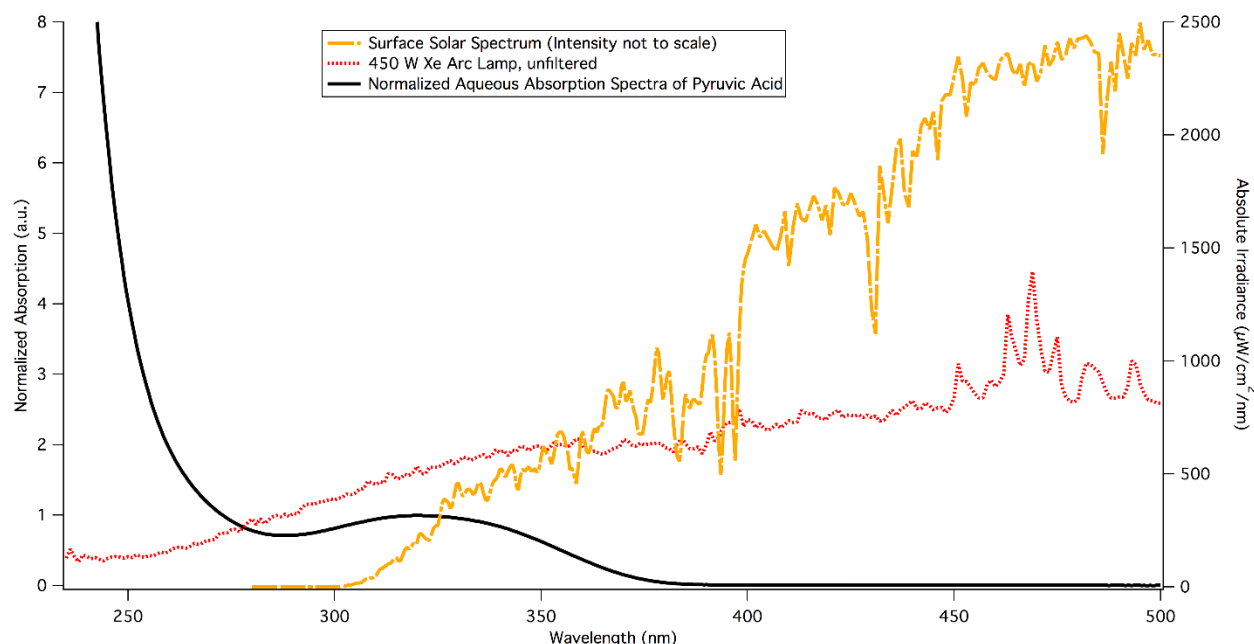


Figure 13. Normalized absorption spectrum of pyruvic acid (black) spectral irradiance (yellow, not to scale),<sup>27</sup> and absolute irradiance of the 450 W Xe arc lamp (red).

### Dark Processing of Pre-Photolysis Solutions

In addition to measuring the ratio of the keto and diol conformers, NMR analysis was also used as well to monitor how much pyruvic acid remained in solution over time at various pH and to examine the concentration of a potential product, zymonic acid, as a function of time. This was necessary because in addition to undergoing photochemistry, pyruvic acid is also known to react to form oligomers in the dark.<sup>28</sup> Zymonic acid (structure shown in Figure 6) as well as

various tautomers and hydrates, including parapyruvic acid are formed even from pure, distilled pyruvic acid, growing in slowly over time. For concentrated aqueous solutions of pyruvic acid it has been observed that this process occurs more rapidly at higher pH.<sup>28</sup> Therefore, to check that these dark processes would not interfere with the interpretation of the photolysis results, NMR of 10 mM pyruvic acid dark solutions were examined over time. The dark solution is a solution of pyruvic acid at the same concentration as the solutions used in photolysis that are not exposed to light so that no photochemistry can occur.

Figure 14 shows the percentage of pyruvic acid in solution over time for a range of pH values. Over the time period studied, there is not a large decrease in pyruvic acid concentration, suggesting that dark processes are not occurring on a large scale. There is some variation in the percentage of pyruvic acid present in solution, with slightly less for higher pH solutions; however, this is a relatively small difference. If anything, it appears as if the percentage of pyruvic acid is increasing over time for the pH 10.46 solution, likely because of the dilute solution conditions. Figure 15 further confirms that the dark processes are not leading to a significant population zymonic acid is not accumulating in the dark reaction, using the closed enol form of zymonic acid as a proxy for all the tautomers and hydrates that exist in aqueous solution. Once again, if anything, it appears that the solution is “purifying” itself slowly with the percentage of zymonic acid appearing to decrease slightly over time. This suggests that any new products identified by mass spectrometry are likely a result of the photochemistry and not dark processes. Aliquots of the pre-photolysis solutions were also kept as controls for comparison to the photolysis solution to confirm this.

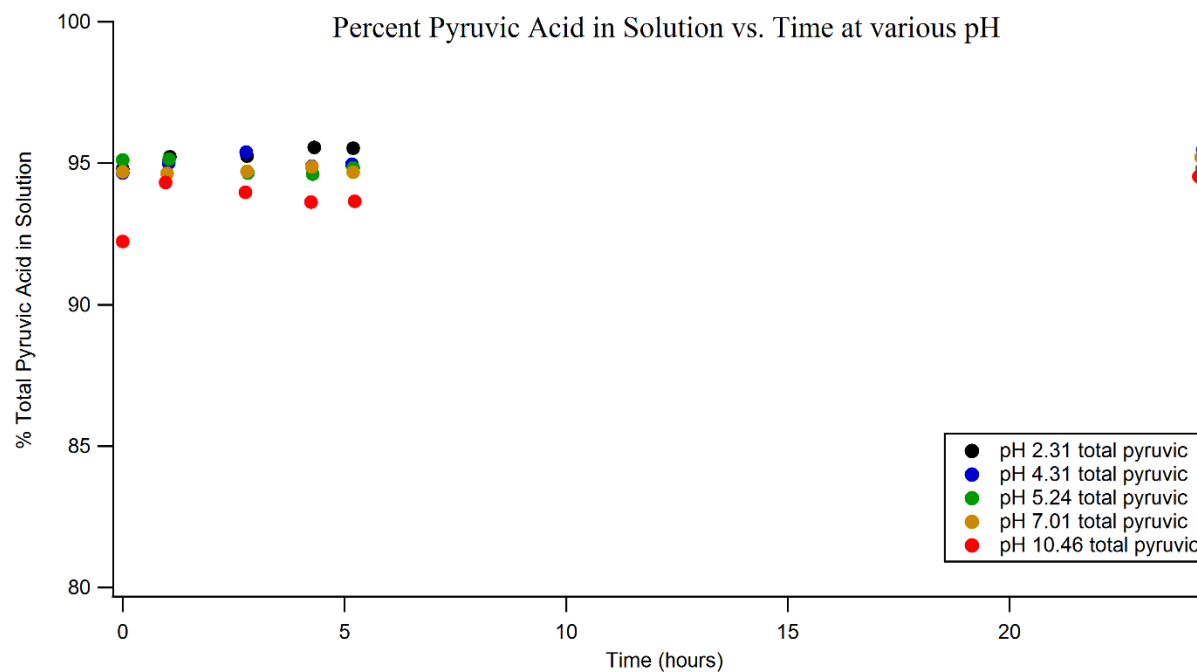


Figure 14. Percent pyruvic acid in solution vs time at various pH

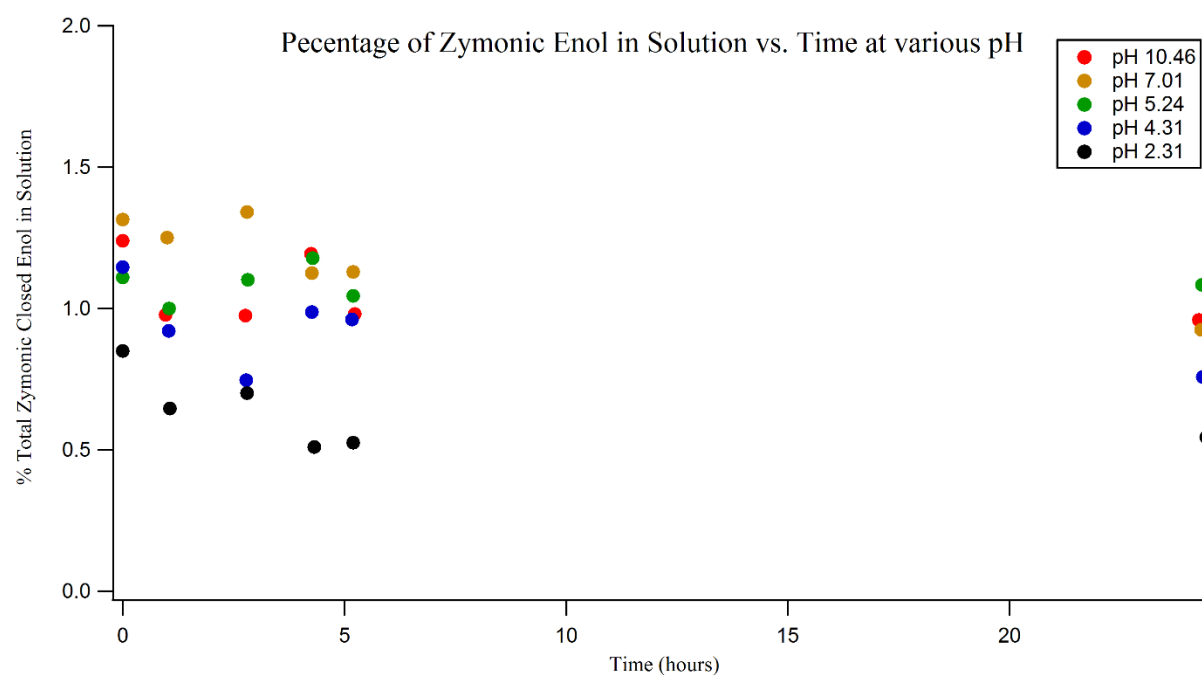


Figure 15. Percentage of zymonic enol in dark solution vs. time

## Photolysis of Pyruvic Acid

After determining that dark reactions are not significant over the reaction timescale, the photolysis of aqueous pyruvic acid was investigated for three different initial pH values, 2 (unadjusted), 6, and 10. Aliquots were saved of the pre-photolysis solution as well as taken every hour of the photolysis. Using these aliquots, the pH was monitored over the course of photolysis and compared to the pre-photolysis solution, yielding an interesting result. The figures below (Figures 16-18) include measurements from the photolysis solutions (aliquots) as well as another vial of the same solution left sitting in the dark to examine if the pH was changing on its own. While small variations in pH were observed for the dark solution over the course of photolysis at all pH values, these changes were smaller than those seen during photolysis. It makes sense that changes in pH would be larger for the photochemical sample where the acid material is being consumed, unlike in the dark samples.

Figure 16 shows a small, but consistent increase in pH during photolysis, changing at a faster rate in the photolysis reaction than the dark reaction. This shows that the pH change during the photolysis is indicative of pyruvic acid depletion because otherwise the same pH would be reached by both dark and photolysis samples. This small increase in pH during photolysis has been observed for pyruvic acid before<sup>12</sup>, and is likely because the products, such as DMTA, are less acidic than pyruvic acid.

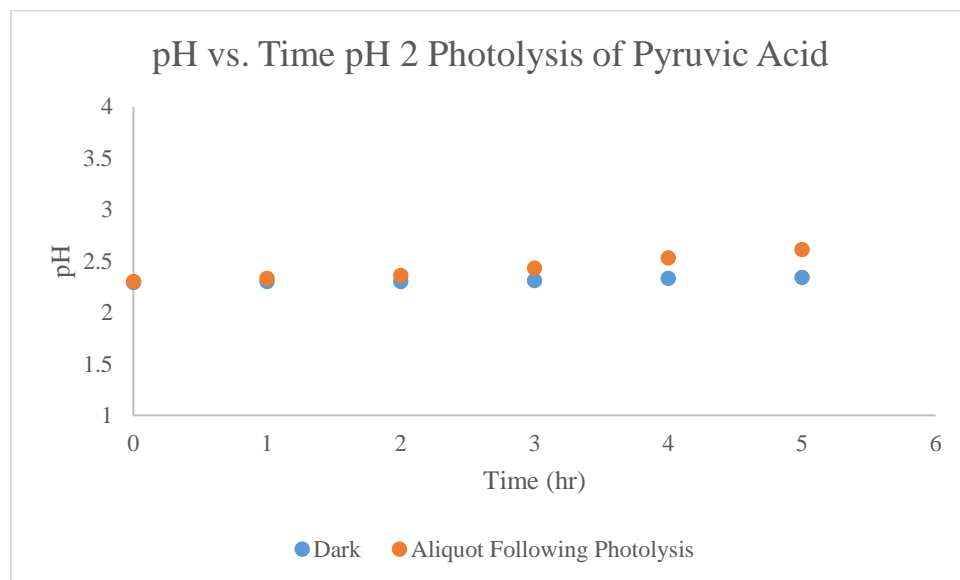
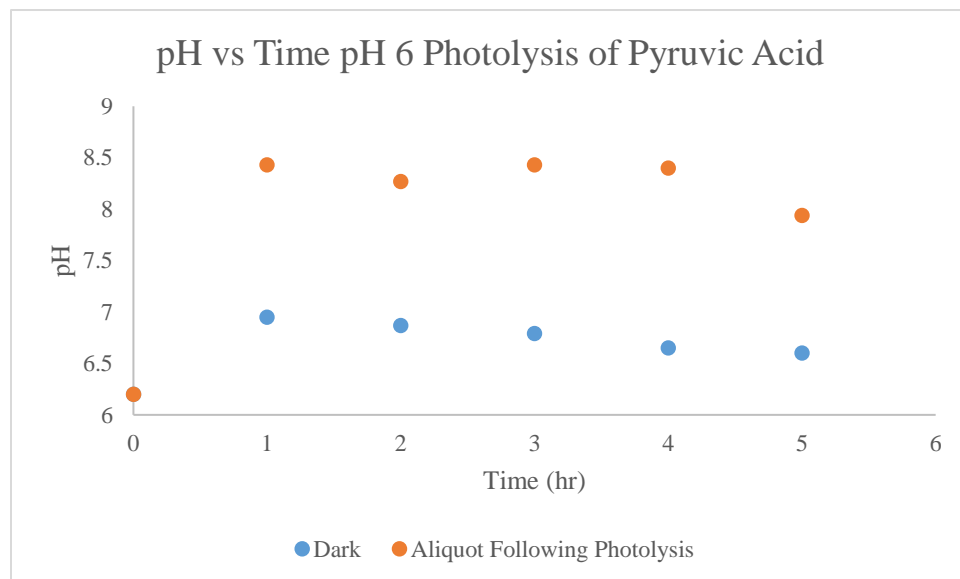


Figure 16. pH vs. time graph for pH 2 photolysis of pyruvic acid

In comparison to the results for the unadjusted solution of pyruvic acid, the pH 6 solutions (Figure 17) shows a much larger change in pH during photolysis, increasing to a pH of ~8. This larger change can be rationalized by referring to the titration curve shown in Figure 9: the solution with initial pH of 6 is within the exponential region for pyruvic acid, meaning a small change in acid concentration will cause a large change in pH. Again, the pH increases over time because the products are less acidic.

As shown in Figure 18, the change in pH observed for the pH 10 solution is again much smaller than for the pH 6 solution, which makes sense because the high pH solution is no longer in the exponential region for pyruvic acid. Interestingly, however, the pH of the high pH solution appears to decrease during photolysis, unlike the low and medium pH solutions. This effect is not easily explained, and this result needs to be further replicated to ensure that this observed decrease in pH is real.



*Figure 17. pH vs. time graph for pH 6 photolysis of pyruvic acid*

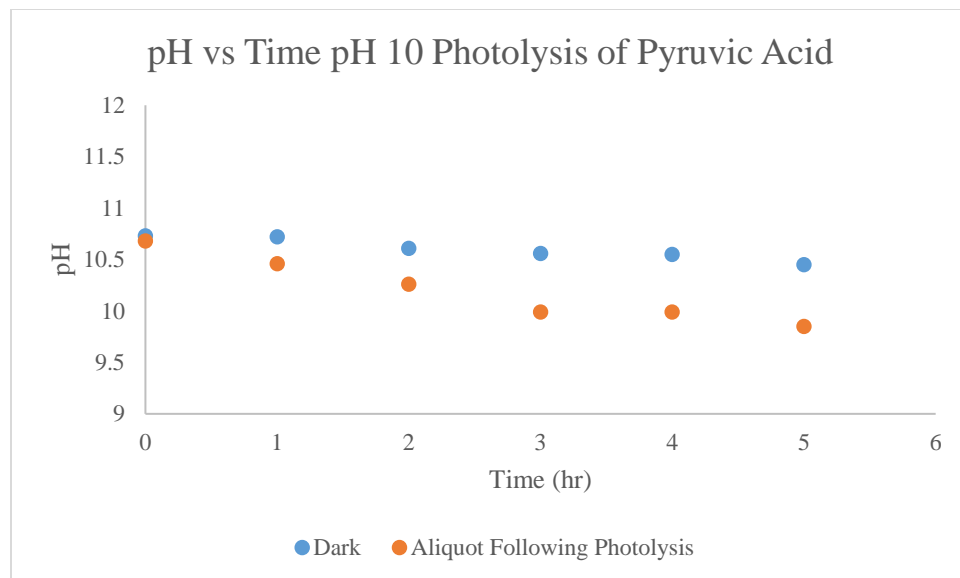


Figure 18. pH vs. time graph for pH 10 photolysis of pyruvic acid

The photolyses of pyruvic acid were also monitored by UV-vis spectroscopy, which was used to obtain qualitative information about the kinetics of reaction as a function of pH. These UV-vis spectra can give insight into the pH dependence of the reaction. As shown in Figure 11 above, the starting absorption for the high pH solution is larger than for the unadjusted pH one, likely because of the higher keto-diol ratio. However, the literature suggests that the kinetics of photolysis are slowed at higher pH,<sup>20</sup> despite this increased absorption.

The spectra in Figure 19 are obtained from aliquots taken as the aqueous pyruvic acid photolysis at unadjusted pH progressed. In these UV-vis spectra for the pH 2 solution, a double isosbestic point is observed. Isosbestic points correspond to the conversion of one of the absorbing components into a different state in a 1:1 ratio. In this case, the isosbestic points indicate the decrease in pyruvic acid and a corresponding increase of an oligomer that also absorbs light.<sup>12, 14</sup> This oligomer has never been identified definitively, but it seems reasonable that it may be DMTA because DMTA is the major observed product under these reaction conditions.



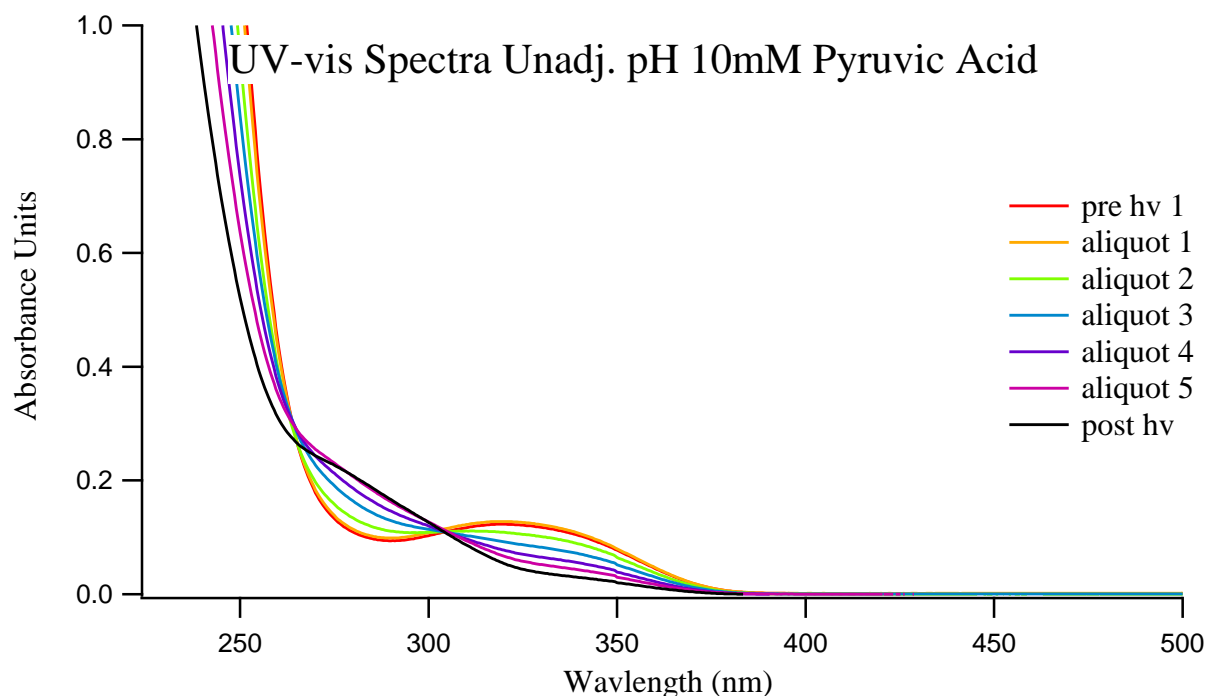


Figure 19. UV-vis spectra of hourly aliquots of the aqueous phase photochemical reaction of pyruvic acid at an unadjusted pH.

Figure 20 shows similar UV-vis spectra that were taken for the pH 10 photolysis samples, with different results from the pH 2 spectra as expected. Notably, a smaller decrease can be observed in absorbance over time compared to the pH 2 spectra. This suggests a difference in the rate of the photolysis reaction as a function of pH. This is consistent with the literature that the rate is slowed as pH increases.<sup>20</sup> And it seems likely that this slow down in kinetics may be due to the decrease in relative amounts of the diol conformer, which is the energetically favored form for hydrogen abstraction.<sup>14</sup> In addition to a qualitative decrease in reaction kinetics, the shape of the spectra also changes. Interestingly, the isosbestic point is no longer observed during photolysis, and the oligomer peak is no longer seen to grow in during photolysis. This suggests that different products are formed during photolysis, resulting in the different shape of the spectra.

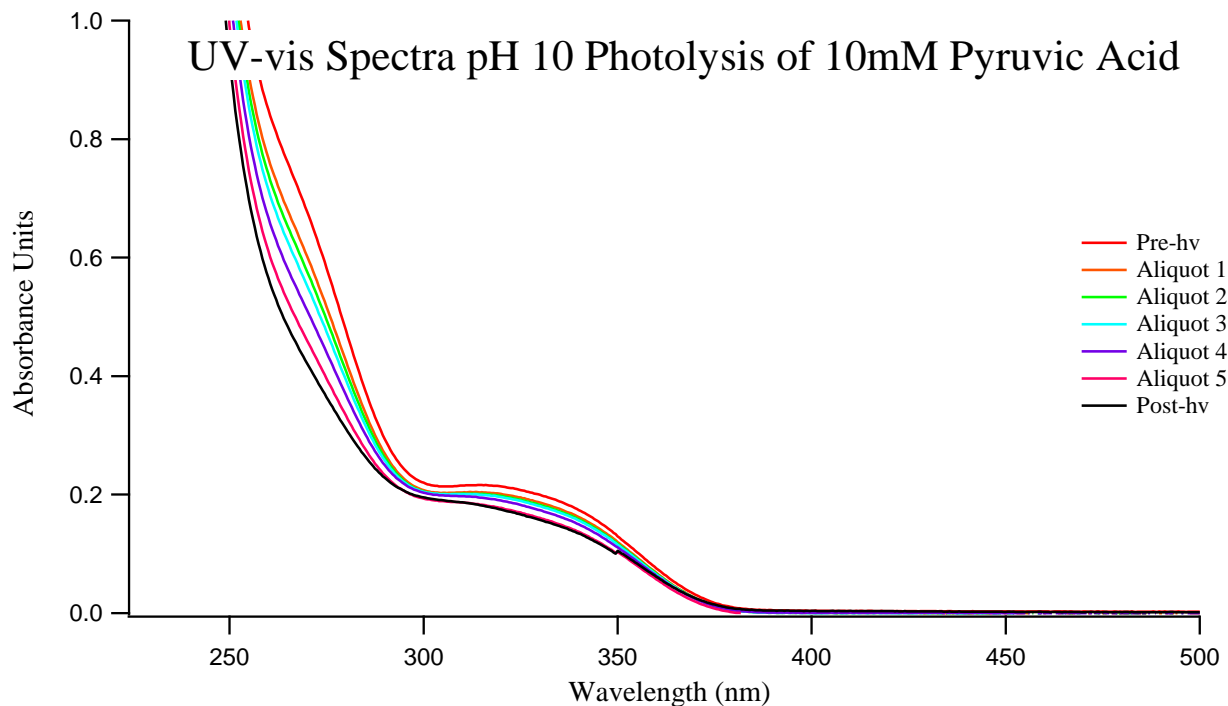
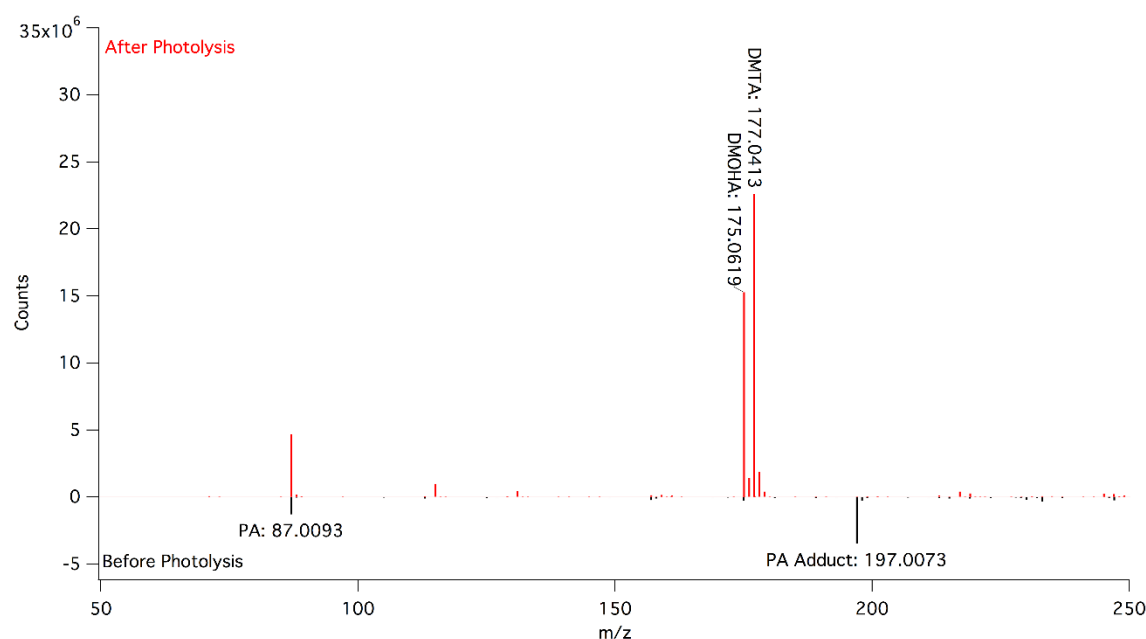


Figure 20. UV-vis spectra of hourly aliquots of the aqueous phase photolysis of pyruvic acid solutions at pH 10.

The variance in absorbance as a function of pH shows that the components of the mixture are changing. After these UV-vis spectra, it seems likely that different branching ratios are followed during photolysis at high pH compared to low pH. To confirm these suspicions mass spectrometry was used to compare the identities of products produced in both the low pH and high pH photolysis. Our mass spectrometry investigation was, however, qualitative, and there is the possibility that any differences in product formation observed in the MS data might be due to differing ionization potential of the products as pH is changed. The differences in the shape of the post-photolysis UV-vis spectra, however, act as confirmation that the product ratios are, in fact, different at high pH and differences in the MS data are likely due to a real shift in branching ratio.

Negative mode electrospray ionization mass spectrometry (ESI<sup>-</sup> MS) of the pyruvic acid photolysis solutions at different pH was used for product identification and qualitative evaluation of the relative ratios of photoproducts. Representative ESI<sup>-</sup> mass spectra of 10 mM pyruvic acid at unadjusted pH (pH 2) before and after photolysis are shown in Figure 21. Under our ionization conditions, only singly-charged species are expected to be observed. As seen in the pre-

photolysis spectrum, a ion corresponding to pyruvic acid (theoretical  $m/z$  of 87.0082) is readily observed. Additionally, there is an ion that corresponds to an adduct of two deprotonated pyruvic acid molecules coordinated to a sodium ion (theoretical  $m/z$  of 197.0062). In the unadjusted pH solutions, sodium is a trace species in solution. The MS data for the unadjusted pH solutions can be compared to that for the pH 10 solutions, shown in Figure 22. In the higher pH solutions, more of the pyruvic adduct with sodium is observed relative to the amount of free pyruvic acid because there is more sodium present because of the addition of NaOH to change the pH of the solution.



*Figure 21. Representative ESI MS of 10 mM pyruvic acid at pH 2 before (black, counts multiplied by -1 for ease of presentation) and after photolysis (red)*

Following photolysis both DMTA (theoretical  $m/z$  of 177.0400) and DMOHA (theoretical  $m/z$  of 175.0607) are observed as photoproducts regardless of the pH of the solution. However, as hypothesized, the ratio of DMTA to DMOHA changes considerably as a function of pH in this experiment. At low pH, more DMTA is produced and at high pH more DMOHA is produced. This is consistent with the idea that at higher pH when there is more keto conformer of pyruvic acid and more of that keto conformer is deprotonated, the reaction pathway that produces parapyruvic acid and ultimately DMOHA is favored. This is because when the keto conformer is deprotonated the methyl group is the only available site for hydrogen abstraction. This shift in branching ratio is also consistent with the slower kinetics observed both in the UV-

vis spectra and in the MS data, where, qualitatively, there appears to be much more starting material remaining in the pH 10 solution after photolysis.

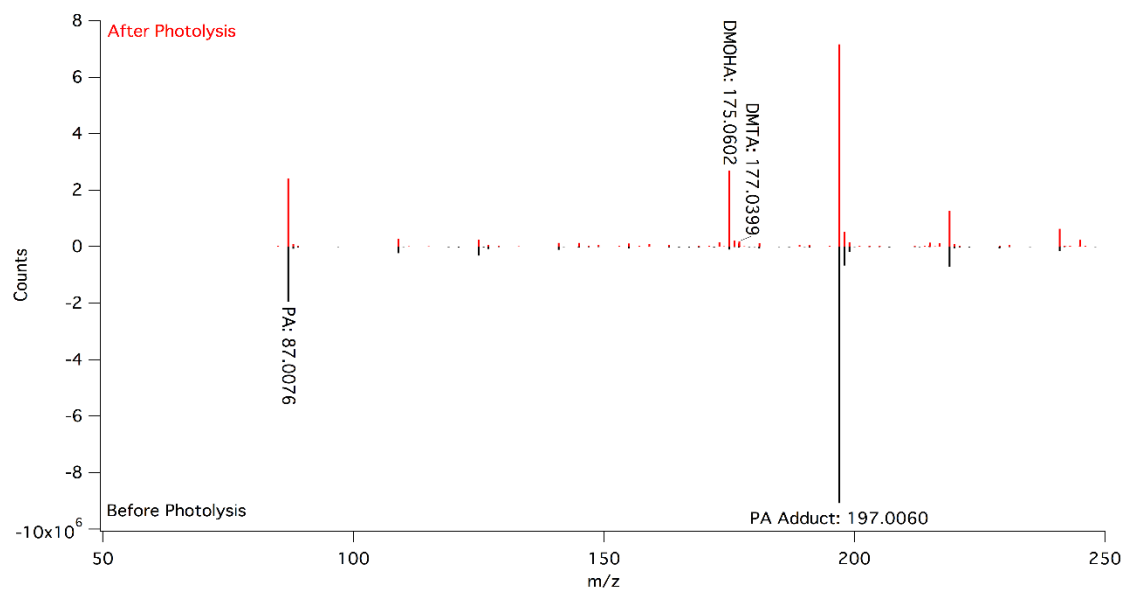


Figure 22. Representative ESI MS of 10 mM pyruvic acid at pH 10 before (black, counts multiplied by -1 for ease of presentation) and after photolysis (red)

## Conclusions and Future Directions

In this work, solutions of  $\alpha$ -keto acids were characterized as a function of pH, and the effect of increased pH on the photochemical reactivity of pyruvic acid was investigated. The effective  $pK_a$  of pyruvic acid and 2-oxooctanoic acid were determined to be  $2.51 \pm 0.05$  and  $2.49 \pm 0.04$ , respectively, suggesting that the length of alkyl chain of  $\alpha$ -keto acids does not have a significant effect on the  $pK_a$ . To confirm this, the acid dissociation constants of other  $\alpha$ -keto acids found in the natural environment will be calculated using iterative fitting of titration data using the extended Debye-Huckel method.

As shown in this work, the photochemistry of pyruvic acid changes significantly as a function of pH. Investigation of this photolysis reaction at high pH had interesting results. As determined by NMR, the keto-diol ratio shifts to favor the keto conformer at high pH, and this shift likely accounts for the relative increase in absorption observed in the UV-vis spectra. Under the dilute conditions used here, dark reactions do not appear to contribute to the difference in

products. The kinetics of reaction appear to decrease at higher pH in agreement with the literature.<sup>20</sup> For the first time, I have shown that the branching ratio also shifts as a function of pH to favor the formation of DMOHA instead of DMTA. These changes due to the acidity of the solution have important implications for the reaction of  $\alpha$ -keto acids in the natural environment, where aqueous environments with very different acidities are found.

In the future, I will extend this study to include longer-tailed  $\alpha$ -keto acids, including 2-OOA. Such longer-tailed species follow the same photochemical mechanisms,<sup>13</sup> but the products formed have longer alkyl chains that are more surface-active. The longer alkyl chain also makes these species less volatile, which increases the importance of understanding their aqueous reactivity. Taken together, this suggests that it is important to account for these reactions as they are likely to contribute to SOA formation. The photolysis of these compounds under atmospherically-relevant conditions can be performed and the results used to evaluate the rates of the reactions of these molecules, especially their potential contributions to SOA formation.

## References

1. Boucher, O.; Randall, D.; Artaxo, P.; Bretherton, C.; Feingold, G.; Forster, P.; Kerminen, V. M.; Kondo, Y.; Liao, H.; Lohmann, U.; Rasch, P.; Satheesh, S. K.; Sherwood, S.; Stevens, B.; Zhang, X. Y., Clouds and Aerosols. In *Climate Change 2013: The Physical Science Basis. Contribution of Working Group I to the Fifth Assessment Report of the Intergovernmental Panel on Climate Change*, Stocker, T. F.; Qin, D.; Plattner, G. K.; Tignor, M.; Allen, S. K.; Boschung, J.; Nauels, A.; Xia, Y.; Bex, V.; Midgley, P. M., Eds. Cambridge Univ. Press, : Cambridge, U.K. and New York, NY, USA, 2013; pp 465-570.
2. Fann, N.; Lamson, A. D.; Anenberg, S. C.; Wesson, K.; Risley, D.; Hubbell, B. J., Estimating the National Public Health Burden Associated with Exposure to Ambient Pm<sub>2.5</sub> and Ozone. *Risk Analysis* **2012**, 32 (1), 81-95.
3. Dockery, D. W.; Pope, C. A.; Xu, X.; Spengler, J. D.; Ware, J. H.; Fay, M. E.; Ferris Jr, B. G.; Speizer, F. E., An Association between Air Pollution and Mortality in Six Us Cities. *New England journal of medicine* **1993**, 329 (24), 1753-1759.
4. Perraud, V.; Bruns, E. A.; Ezell, M. J.; Johnson, S. N.; Yu, Y.; Alexander, M. L.; Zelenyuk, A.; Imre, D.; Chang, W. L.; Dabdub, D.; Pankow, J. F.; Finlayson-Pitts, B., Nonequilibrium Atmospheric Secondary Organic Aerosol Formation and Growth. *Proc. Natl. Acad. Sci.* **2012**, 109 (8), 2836-2841.
5. Vaida, V., Atmospheric Radical Chemistry Revisited. *Science* **2016**, 353 (6300), 650-650.
6. Ellison, G. B.; Tuck, A. F.; Vaida, V., Atmospheric Processing of Organic Aerosols. *J. Geophys. Res. Atmos.* **1999**, 104 (D9), 11633-11641.
7. Renard, P.; Reed Harris, A. E.; Rapf, R. J.; Rainer, S.; Demelas, C.; Coulomb, B.; Quivet, E.; Vaida, V.; Monod, A., Aqueous Phase Oligomerization of Methyl Vinyl Ketone by Atmospheric Radical Reactions. *J. Phys. Chem. C* **2014**, 118, 29421-29430.
8. Dobson, C. M.; Ellison, G. B.; Tuck, A. F.; Vaida, V., Atmospheric Aerosols as Prebiotic Chemical Reactors. *Proc. Natl. Acad. Sci.* **2000**, 97 (22), 11864-11868.
9. Hallquist, M.; Wenger, J. C.; Baltensperger, U.; Rudich, Y.; Simpson, D.; Claeys, M.; Dommen, J.; Donahue, N. M.; George, C.; Goldstein, A. H.; Hamilton, J. F.; Herrmann, H.; Hoffmann, T.; Iinuma, Y.; Jang, M.; Jenkin, M. E.; Jimenez, J. L.; Kiendler-Scharr, A.; Maenhaut, W.; McFiggans, G.; Mentel, T. F.; Monod, A.; Prévôt, A. S. H.; Seinfeld, J. H.; Surratt, J. D.; Szmigielski, R.; Wildt, J., The Formation, Properties and Impact of Secondary Organic Aerosol: Current and Emerging Issues. *Atmos. Chem. Phys.* **2009**, 9 (14), 5155-5236.
10. Griffith, E. C.; Rapf, R. J.; Shoemaker, R. K.; Carpenter, B. K.; Vaida, V., Photoinitiated Synthesis of Self-Assembled Vesicles. *J. Am. Chem. Soc.* **2014**, 136 (10), 3784-3787.
11. Rapf, R. J.; Perkins, R. J.; Carpenter, B. K.; Vaida, V., Mechanistic Description of Photochemical Oligomer Formation from Aqueous Pyruvic Acid. *J. Am. Chem. Soc.* **2017**, Submitted.
12. Reed Harris, A. E.; Ervens, B.; Shoemaker, R. K.; Kroll, J. A.; Rapf, R. J.; Griffith, E. C.; Monod, A.; Vaida, V., Photochemical Kinetics of Pyruvic Acid in Aqueous Solution. *J. Phys. Chem. A* **2014**, 118 (37), 8505-8516.
13. Rapf, R. J.; Perkins, R. J.; Yang, H.; Miyake, G. M.; Carpenter, B. K.; Vaida, V., Photochemical Synthesis of Oligomeric Amphiphiles from Alkyl Oxoacids in Aqueous Environments. *J. Am. Chem. Soc.* **2017**, Submitted.

14. Griffith, E. C.; Carpenter, B. K.; Shoemaker, R. K.; Vaida, V., Photochemistry of Aqueous Pyruvic Acid. *Proc. Natl. Acad. Sci.* **2013**, *110* (29), 11714-11719.
15. Rapf, R. J.; Vaida, V., Sunlight as an Energetic Driver in the Synthesis of Molecules Necessary for Life. *Phys. Chem. Chem. Phys.* **2016**, *18* (30), 20067-20084.
16. Rapf, R. J.; Vaida, V., Sunlight as an Energetic Driver in the Synthesis of Molecules Necessary for Life. *Phys. Chem. Chem. Phys.* **2016**.
17. Altieri, K. E.; Carlton, A. G.; Lim, H.-J.; Turpin, B. J.; Seitzinger, S. P., Evidence for Oligomer Formation in Clouds: Reactions of Isoprene Oxidation Products. *Environ. Sci. Technol.* **2006**, *40* (16), 4956-4960.
18. Mellouki, A.; Mu, Y. J., On the Atmospheric Degradation of Pyruvic Acid in the Gas Phase. *J. Photochem. Photobiol., A* **2003**, *157* (2-3), 295-300.
19. Larsen, M. C.; Vaida, V., Near Infrared Photochemistry of Pyruvic Acid in Aqueous Solution. *J. Phys. Chem. A* **2012**, *116*, 5840-5846.
20. Leermakers, P. A.; Vesley, G. F., Photolysis of Pyruvic Acid in Solution. *J. Org. Chem.* **1963**, *28* (4), 1160-1161.
21. Maroń, M. K.; Takahashi, K.; Shoemaker, R. K.; Vaida, V., Hydration of Pyruvic Acid to Its Geminal-Diol, 2, 2-Dihydroxypropanoic Acid, in a Water-Restricted Environment. *Chem. Phys. Lett.* **2011**, *513* (4), 184-190.
22. Harris, D. C., *Quantitative Chemical Analysis*. 7th ed.; W.H. Freeman and Company: New York, 2007.
23. Papanastasiou, G.; Ziogas, I., Simultaneous Determination of Equivalence Volumes and Acid Dissociation Constants from Potentiometric Titration Data. *Talanta* **1995**, *42* (6), 827-836.
24. Pocker, Y.; Meany, J. E.; Nist, B. J.; Zadorojny, C., Reversible Hydration of Pyruvic Acid. I. Equilibrium Studies. *J. Phys. Chem.* **1969**, *73* (9), 2879-2882.
25. Pedersen, K. J., The Dissociation Constants of Pyruvic and Oxaloacetic Acid. *Acta Chem. Scand.* **1952**, *6* (2), 243-256.
26. Xu, H.; Du, N.; Song, Y.; Song, S.; Hou, W., Vesicles of 2-Ketooctanoic Acid in Water. *Soft Matter* **2017**, DOI: 10.1039/C6SM02665F.
27. Gueymard, C. A., Parameterized Transmittance Model for Direct Beam and Circumsolar Spectral Irradiance. *Solar Energy* **2001**, *71* (5), 325-346.
28. Perkins, R. J.; Shoemaker, R. K.; Carpenter, B. K.; Vaida, V., Chemical Equilibria and Kinetics in Aqueous Solutions of Zymonic Acid. *J. Phys. Chem. A* **2016**, *120* (51), 10096-10107.